Hydrolysis of DNA and RNA by lanthanide ions: mechanistic studies leading to new applications

Makoto Komiyama,[*a] **Naoya Takeda**[a] **and Hidemi Shigekawa**[b]

[a] *Department of Chemistry and Biotechnology, Graduate School of Engineering, The University of Tokyo, Hongo, Tokyo 113-8656 Japan. E-mail: mkomi@chembio.t.u-tokyo.ac.jp*

[b] *Institute of Applied Physics and Center for Tsukuba Advanced Research Alliance (TARA), University of Tsukuba, Tsukuba, Ibaraki 305-8573, Japan*

A few years ago, the remarkable catalytic activity of lanthanide ions for the hydrolysis of nucleic acids was discovered. With Ce^{IV}, DNA was hydrolysed under physiological conditions. For RNA hydrolysis, the last three lanthanide ions (Tm^{III}, Yb^{III}, and Lu^{III}) are superb. Furthermore, artificial restriction enzymes for site-selective scission of DNA and RNA, essential tools for the future biotechnology, have been prepared by using the lanthanide complexes. The present article emphasizes the mechanistic aspects of the catalyses of these metal ions. Both DNA hydrolysis and RNA hydrolysis involve the cooperation of acid catalysis (by metal ion and/or metal-bound water) and base catalysis (by metal-bound hydroxide). The magnitudes of contributions of these catalyses, as well as the positions where they work, are primarily governed by the relative height of the energy-barrier for the formation of the pentacoordinated intermediate and that for its breakdown. The following conclusions have been obtained on the basis of various kinetic and spectroscopic evidence: (1) for the hydrolysis of both DNA and RNA, the catalytically active species are dinuclear hydroxo-clusters, (2) Ce^{IV} enormously activates DNA and promotes the formation of the pentacoordinated intermediate, and (3) the catalysis for RNA hydrolysis is mainly ascribed to the promotion of breakdown of the pentacoordinated intermediate.

Introduction

Non-enzymatic hydrolysis of DNA and RNA has attracted much interest, mainly because it is essential for further developments in biotechnology, molecular biology, therapy, and related fields.[1] In current biotechnology, the DNA of bacteria and viruses is manipulated using naturally-occurring enzymes. In the near future, however, we must deal with the DNA of higher animals and plants in order to widen the scope of applications. Is the currently employed technology directly applicable there? The answer is 'No'. First, the genomes of higher species are so large that the sequence-specificity of the restriction enzymes found in nature is too low to cut them solely at the desired site (most of them recognize a specific sequence composed of 4 or 6 DNA-bases).[2] Second, there are no natural enzymes showing sufficient sequence-specificity in RNA scission. Thus, artificial enzymes, which selectively hydrolyse DNA and RNA at the target position with a desired specificity, are crucially important. They may also be valuable tools for therapy, regulation of cell-growth, and other applications.

In order to prepare these artificial enzymes, catalysts for the scission of DNA and RNA are necessary. However, the phosphodiester linkages in DNA are enormously stable, and (until recently) could not be hydrolysed without using natural enzymes.[3,4] Non-enzymatic hydrolysis of RNA was also difficult. Several years ago, however, the remarkable catalytic activity of the lanthanide ions was discovered, and both DNA and RNA were for the first time hydrolysed at reasonable rates under physiological conditions.[5–7] The Ce^{IV} ion is the most active for DNA hydrolysis,[8,9] whereas Tm^{III}, Yb^{III} and Lu^{III} (the last three lanthanide ions) are quite effective for RNA hydrolysis.[10] The acceleration by these metal ions is as large as 10^8–10^{12} fold. Interestingly, these enormous activities are restricted to the lanthanide ions. Furthermore, artificial enzymes

Professor Makoto Komiyama was born in 1947 in Utsunomiya, Japan. After graduated from the University of Tokyo, he entered the Graduate School of this University, where he got his Ph.D. in 1975. After working in the USA as a postdoctoral fellow for Professor Myron L. Bender at Northwestern University, he got the position of Assistant Professor at the University of Tokyo in 1979. In 1987, he became an Associate Professor at the University of Tsukuba, and, since 1992, has been a full Professor of the University of Tokyo. His research areas involves bioorganic and bioinorganic chemistry (especially DNA and RNA hydrolysis), host–guest chemistry (cyclodextrins), functional polymers, and others. He received Awards for Young Scientists from the Chemical Society of Japan, the Japan IBM Science Award, an Award from the Rare Earth Society of Japan, and the Inoue Prize for Science.

Dr Naoya Takeda was born in 1968 in Chiba, Japan. Following his undergraduate education at the University of Tokyo, he obtained his Ph.D. from the University in 1998 under the

supervision of Professor M. Komiyama. After working as an assistant staff member at the National Institute for Advanced Interdisciplinary Research, he is currently doing his post-doctoral work as a JSPS Research Fellow at the University of Tokyo. His research interests include bioorganic and bio-inorganic chemistry.

Professor Hidemi Shigekawa was born in 1955 in Hiroshima, Japan. After graduated from the University of Tokyo, he entered the Graduate School of the University, and got a position of Assistant Professor there in 1980. After getting his Ph.D. in 1986, he worked at the Brook Haven National Laboratory (1987–1988) using the synchrotron radiation source, as a Postdoctoral Fellow for Dr J. Rowe of Bell Labs. In 1989, he became a lecturer at the University of Tsukuba, and has been an Associate Professor there since 1993. His main research is in the field of surface science using scanning tunneling microscopy and related techniques. He was awarded the Paper Award from the Surface Science Society of Japan in 1991 and 1998.

for site-selective scission of DNA and RNA were prepared by conjugating the lanthanide complexes to DNA oligomers (the sequence-recognizing moieties) (Fig. 1).[11,12] The DNA and
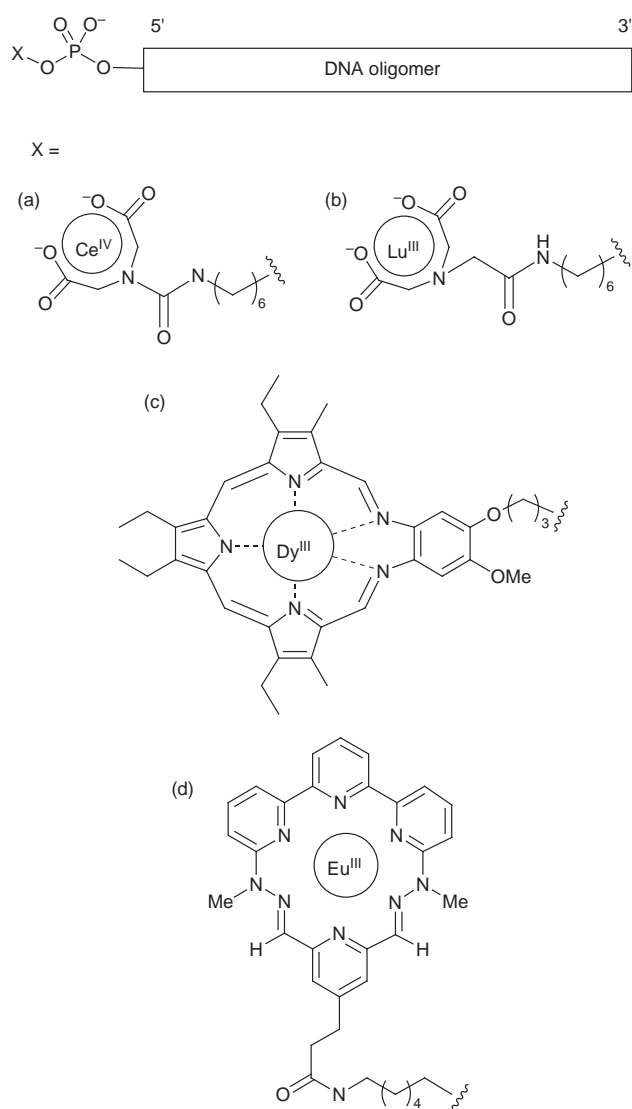

Fig. 1 Typical artificial enzymes for sequence-selective scission of (*a*) DNA and (*b*)–(*d*) RNA.

RNA fragments, obtained *via* scission, can be transformed into substrates for enzymatic manipulation. The synergy between lanthanide catalysis and biotechnology is straightforward.[13] A new era is imminent.

This paper focuses on the mechanistic aspects of the lanthanide catalysis for the hydrolysis of DNA and RNA. The following points are clarified on the basis of various kinetic and spectroscopic evidence: (a) what are the catalytically active species?, (b) where do the catalyses work in the course of the reactions?, and (c) why are the lanthanide ions highly active? The mechanisms of the catalyses for DNA and RNA are compared with each other, and also with those for the RNA hydrolysis by dinuclear complexes of non-lanthanide ions. The conclusions obtained here should pave the way to the rational design of still more active catalysts and also to versatile applications of these novel catalyses.

1 DNA hydrolysis by Ce^{IV}

1.1 Survey of the previous studies

The following features of Ce^{IV}-induced DNA hydrolysis have been already documented.[9]

(1) The DNA scission proceeds totally *via* the hydrolysis of phosphodiester linkages, without concurrent oxidative cleavage of the deoxyribose residues.

(2) At pH 7 and 50 °C, the half-life of the phosphodiester linkage in DNA is reduced to a few hours. The acceleration by Ce^{IV} is more than 10^{11} fold.

(3) The catalytically active species is formed from tetravalent Ce ion(s).

(4) Molecular oxygen is not necessary for the catalysis. Only when Ce^{III} salts (*e.g.* CeCl$_3$) are used as the catalysts, is molecular oxygen required to oxidize Ce^{III} to the catalytically active Ce^{IV}.

(5) The rate of DNA hydrolysis is almost constant from pH 2 to pH 8.5.

(6) The nucleic acid bases do not directly participate in the catalysis (the rate of DNA hydrolysis is almost independent of them).

(7) The reaction is accompanied by a notable D$_2$O solvent isotope effect ($k_{H_2O}/k_{D_2O} = 2.2$–2.4), showing a rate-limiting proton-transfer.

1.2 The rate-limiting step for DNA hydrolysis

The hydrolysis of DNA proceeds as a two-step reaction (Fig. 2). In the first step, a nucleophile (*e.g.* hydroxide ion) attacks the phosphorus atom, forming a pentacoordinated intermediate. In the second step, the 5′-OH of 2′-deoxyribonucleotide is removed from the phosphorus atom through the scission of the P–O bond [in non-enzymatic hydrolysis, the P–O(3′) scission can also take place]. In order to accelerate the whole reaction, the catalysts must promote the rate-limiting step. Unfortunately, however, it was not known which step is rate-limiting. Thus, the DNA analogues in Fig. 3, which possess better leaving groups
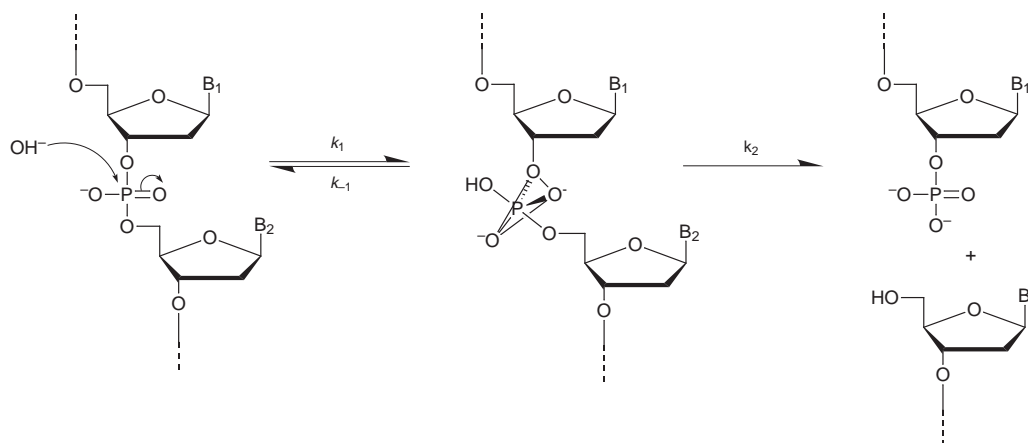

Fig. 2 The reaction pathway of DNA hydrolysis.

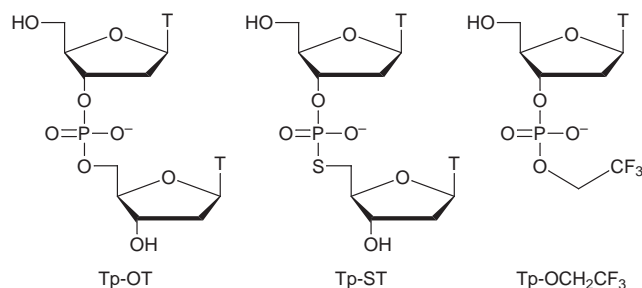than DNA, were prepared as probes, and their hydrolysis rates were compared with the value for the native DNA.[14]

Fig. 3 DNA analogues possessing better leaving groups, as the probes of the rate-limiting step.

(1) Ce^{IV}-induced DNA hydrolysis. When the 5′-O atom of the thymidine in thymidylyl(3′–5′)thymidine (Tp-OT) is replaced with an S atom (the leaving group is changed from T-O⁻ to T-S⁻), the dinucleotide analog (Tp-ST) is hydrolysed by Ce^{IV} around 1000 fold faster than is Tp-OT. The rate constants are 1.7×10^1 and 2.0×10^{-2} h⁻¹, respectively, when $[Ce^{IV}]_0$ = 10 mM at pH 7 and 30 °C. Similarly, the hydrolysis of Tp-OCH₂CF₃ is 75 fold faster than that of Tp-OT. The rate of hydrolysis monotonically increases with decreasing pK_a of the leaving group (the pK_as of T-SH, CF₃CH₂OH, and T-OH are around 11, 13, and 15, respectively). Apparently, the second-step (the scission of the P–O bond) is rate-limiting [the energy diagram is presented by the solid line in Fig. 4(a)]. If the first step were to be rate-limiting, the analogues should be hydrolysed at the same (or comparable) rate as Tp-OT.[15]

By using this result, the rate constant k_{obs} for the overall reaction in Fig. 2 is expressed by eqn. (1). The reaction involves the pre-equilibrium formation of the pentacoordinated intermediate.

$$k_{obs} = k_1 k_2 / k_{-1} \qquad (1)$$

Accordingly, the hydrolysis of DNA is accelerated by (a) the increase in k_2 (promotion of the second-step) and/or (b) the increase in k_1/k_{-1} (stabilization of the pentacoordinated intermediate, with respect to the initial state). The activation free energy for the whole reaction ($\Delta G^{\ddagger}$) is the sum of ΔG_1 (the difference between the initial state and the pentacoordinated intermediate) and $\Delta G_2^{\ddagger}$ (the difference between the intermediate and the second-energy barrier).

The trivalent lanthanide ions also hydrolyse DNA, although the activities are far smaller ($> 10^3$ fold) than that of Ce^{IV}. Here, the second step is also rate-limiting. In contrast, non-lanthanide ions such as Mg^{II}, Zn^{II}, Co^{II}, Al^{III}, and Fe^{III} show no measurable catalysis under the same conditions.

(2) Alkaline hydrolysis. DNA is so stable that it is not hydrolysed at measurable rates even in highly alkaline solutions (*e.g.* in 1 M NaOH at 50 °C). Thus, the direct evaluation of the shape of the energy diagram using the probes in Fig. 3 has been unsuccessful.

However, the following argument shows that the energy diagram is almost symmetric, with respect to the position of the pentacoordinated intermediate: see the dotted line in Fig. 4(a). In the forward reaction of DNA hydrolysis, hydroxide ion is the nucleophile and the alkoxide ion of 5′-OH is the leaving group. In the backward reaction, the hydroxide ion and the alkoxide ion exchange positions. Since the pK_as of the conjugate acids of the hydroxide ion and the alkoxide ion are almost the same, their potentials as nucleophiles and the leaving groups are comparable.

1.3 Which step is promoted by the Ce^{IV} ion?

The Ce^{IV} ion accelerates DNA hydrolysis by 10^{11} fold or more, and thus the second step of the reaction must be promoted by this magnitude [see the energy diagrams in Fig. 4(a)]. Nevertheless, this step still remains rate-limiting in the whole reaction. Apparently, the first step is also accelerated by the Ce^{IV} ion to a similar (or greater) degree (otherwise, this step should become rate-limiting). The difference in the activation free energies between these two steps is not large. The pentacoordinated intermediate should also be stabilized by the metal ion.

As described later, the catalysis by Ce^{IV} is mainly ascribed to the decrease in ΔG_1, which is associated with the activation of the DNA. Note that the decrease in ΔG_1 necessarily lowers the height of the second barrier (with respect to the initial state), since $\Delta G^{\ddagger} = \Delta G_1 + \Delta G_2^{\ddagger}$.

1.4 Catalytically active species for the DNA hydrolysis

The Ce^{IV} ions form complex metal hydroxide gels when the pH is greater than 4. These heterogeneous systems are inappropriate for detailed kinetic analysis. However, it has been found that homogeneous mixtures can be obtained under highly acidic conditions (pH < 2.5).[16] Significantly, these mixtures have almost the same catalytic activity as the metal hydroxide gel (the hydrolysis of single-stranded DNA at pH 2 is only a few
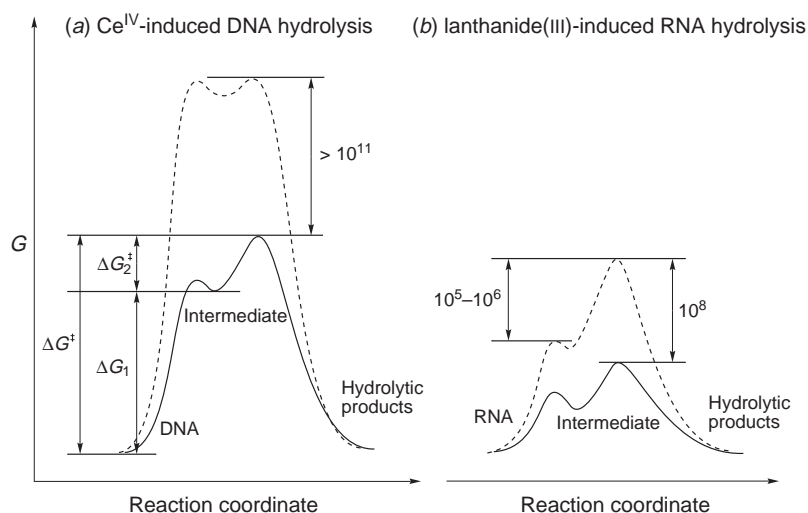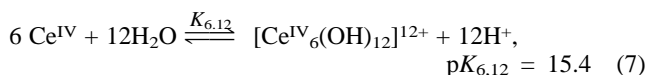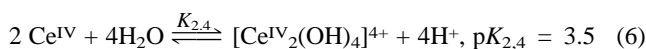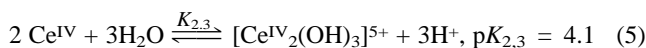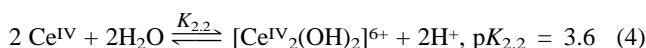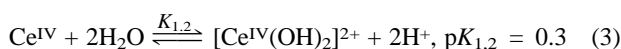

Fig. 4 Energy diagrams for (*a*) Ce^{IV}-induced DNA hydrolysis and (*b*) lanthanide(III)-induced RNA hydrolysis. The dotted lines show the diagrams for the corresponding alkaline hydrolysis.

fold slower than that at pH 7). Moreover, the concentrations of all the Ce^{IV}-derived species therein can be calculated using the equilibrium constants in the literature.[17] Thus, the catalytically active species for DNA hydrolysis in these homogeneous solutions have been investigated.[18,19]

(1) Hydrolysis of cyclic adenosine 3′,5′-monophosphate (cAMP). The hydrolysis of cAMP has many common features with DNA hydrolysis. First, both reactions are enormously (10^{11}–10^{12} fold) promoted by Ce^{IV}.[20] Second, the catalytic activity of Ce^{IV} is far greater than that of any other catalyst. Thirdly, both of the reactions proceed *via* the attack by OH^- (or H_2O) as external nucleophile. The six-membered cyclic phosphodiester in cAMP is activated by strain and is much more readily hydrolysed than the non-cyclic linkage in DNA. A variety of fundamental information on Ce^{IV}-induced DNA hydrolysis can be obtained from cAMP hydrolysis.[18]

In the reaction mixtures, six equilibria [eqn. (2)–(7)] hold.[17]

$$Ce^{IV} + H_2O \xrightleftharpoons{K_{1,1}} [Ce^{IV}(OH)]^{3+} + H^+, \ pK_{1,1} = 1.1 \quad (2)$$

$$Ce^{IV} + 2H_2O \xrightleftharpoons{K_{1,2}} [Ce^{IV}(OH)_2]^{2+} + 2H^+, \ pK_{1,2} = 0.3 \quad (3)$$

$$2\,Ce^{IV} + 2H_2O \xrightleftharpoons{K_{2,2}} [Ce^{IV}_2(OH)_2]^{6+} + 2H^+, \ pK_{2,2} = 3.6 \quad (4)$$

$$2\,Ce^{IV} + 3H_2O \xrightleftharpoons{K_{2,3}} [Ce^{IV}_2(OH)_3]^{5+} + 3H^+, \ pK_{2,3} = 4.1 \quad (5)$$

$$2\,Ce^{IV} + 4H_2O \xrightleftharpoons{K_{2,4}} [Ce^{IV}_2(OH)_4]^{4+} + 4H^+, \ pK_{2,4} = 3.5 \quad (6)$$

$$6\,Ce^{IV} + 12H_2O \xrightleftharpoons{K_{6,12}} [Ce^{IV}_6(OH)_{12}]^{12+} + 12H^+,$$
$$pK_{6,12} = 15.4 \quad (7)$$

Thus, the equilibrium concentrations of all the Ce^{IV}-derived species (Ce^{4+}, $[Ce^{IV}(OH)]^{3+}$, $[Ce^{IV}(OH)_2]^{2+}$, $[Ce^{IV}_2(OH)_2]^{6+}$, $[Ce^{IV}_2(OH)_3]^{5+}$, $[Ce^{IV}_2(OH)_4]^{4+}$, and $[Ce^{IV}_6(OH)_{12}]^{12+}$) are evaluated by using the $K_{1,1}$, $K_{1,2}$, $K_{2,2}$, $K_{2,3}$, $K_{2,4}$, and $K_{6,12}$ values. As depicted in Fig. 5, the pH–rate constant profile (the
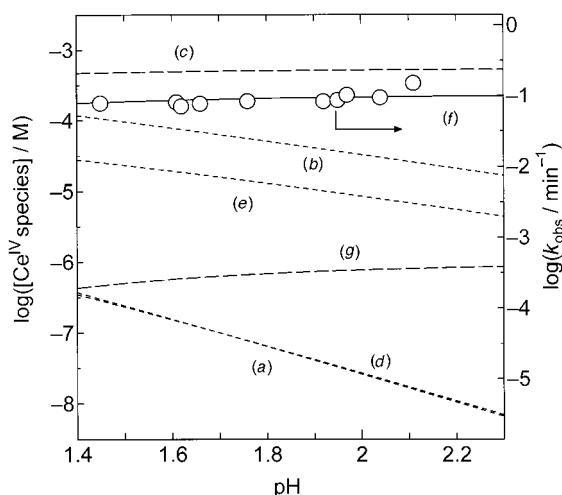
Fig. 5 The pH–rate constant profile for the cAMP hydrolysis by $Ce(NH_4)_2(NO_3)_6$ (10 mM) at 30 °C. The open circles are the experimental points. The equilibrium concentrations of the Ce^{IV}-derived species, calculated by using the K values in eqn. (2)–(7), are presented by the curved lines: (a) Ce^{4+}, (b) $[Ce^{IV}(OH)]^{3+}$, (c) $[Ce^{IV}(OH)_2]^{2+}$, (d) $[Ce^{IV}_2(OH)_2]^{6+}$, (e) $[Ce^{IV}_2(OH)_3]^{5+}$, (f) $[Ce^{IV}_2(OH)_4]^{4+}$, (g) $[Ce^{IV}_6(OH)_{12}]^{12+}$.

open circles) fits reasonably well the theoretical lines for the concentrations of $[Ce^{IV}(OH)_2]^{2+}$ [line (c)], $[Ce^{IV}_2(OH)_4]^{4+}$ [line (f)], and $[Ce^{IV}_6(OH)_{12}]^{12+}$ [line (g)]. These three species are the candidates for the catalytically active species. Note that the shapes of these lines are unanimously determined by the K values, whereas their positions (with respect to the right-hand

side ordinate) can be moved vertically by changing the catalytic rate constants of the corresponding species.

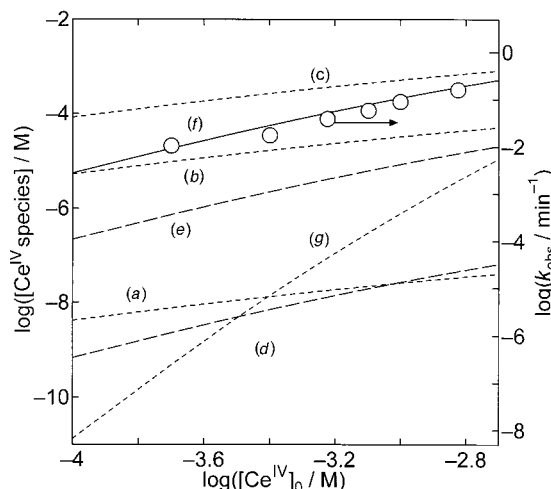In Fig. 6, the hydrolysis rate is plotted *vs.* [$Ce^{IV}(NH_4)_2$-

Fig. 6 The plots of the rate of cAMP hydrolysis *vs.* $[Ce(NH_4)_2(NO_3)_6]_0$ at pH 2.0 and 30 °C. The open circles are the experimental points, whereas the curved lines show the equilibrium concentrations of the corresponding species (see Fig. 5).

$(NO_3)_6]_0$. The experimental points agree well with the theoretical lines for $[Ce^{IV}_2(OH)_2]^{6+}$ [line (d)], $[Ce^{IV}_2$-$(OH)_3]^{5+}$ [line (e)], and $[Ce^{IV}_2(OH)_4]^{4+}$ [line (f)]. Thus, only $[Ce^{IV}_2(OH)_4]^{4+}$ satisfies the results in both Figs. 5 and 6. This tetracationic bimetallic hydroxo cluster is the active species for the remarkable hydrolysis of cAMP.

(2) DNA hydrolysis. The Ce^{IV}-induced DNA hydrolysis has been analyzed in acidic solutions (pH 1.5–2.5) at 50 °C, exactly as described above for the cAMP hydrolysis.[19] It has been concluded that $[Ce^{IV}_2(OH)_4]^{4+}$ is also the active species. Of all the Ce^{IV} ions in the mixtures, only a small portion (20–30%) forms this bimetallic hydroxo-cluster (most of the rest exists as $[Ce^{IV}(OH)_2]^{2+}$), yet this species governs the whole reaction. Its catalytic activity is overwhelmingly greater than those of the other species. The cooperation of the two Ce^{IV} ions in the cluster is strongly indicated (*vide infra*).

From the viewpoints of biological and other practical applications, DNA hydrolysis at around pH 7 is the most important. In these mixtures, $[Ce^{IV}_2(OH)_4]^{4+}$ further aggregates, forming complicated gels. The bimetallic hydroxo clusters in the gels are the active species for DNA hydrolysis.

1.5. Activation of DNA by the Ce^{IV} ion

Why is Ce^{IV} ion highly effective for DNA hydrolysis? Why are the phosphodiester residues significantly activated by this metal ion? Do its f-orbitals play a significant role in the catalysis? In order to answer these questions, core-level photoelectron spectroscopy,[21] as well as EXAFS (extended X-ray absorption fine structure) and XANES (X-ray absorption near edge structure) measurements[22] were carried out. To simplify the analysis, diphenyl phosphate (DPP) was used as the specimen, in place of DNA.[23]

(1) Enormous electron-withdrawal from the phosphate by Ce^{IV}. Fig. 7 presents the core-level spectra for the $2p$ orbitals of the phosphorus atom of DPP in various lanthanide complexes. The electron-withdrawal by the metal ions from the phosphodiester linkage (and thus from the phosphorus atom), if any, is observed as the increase in the binding energy. It has been found that the binding energy of the orbitals in the Ce^{IV} complex is considerably greater than those for the complexes with La^{III}, Eu^{III}, Lu^{III}, and other non-lanthanide ions. Appar-
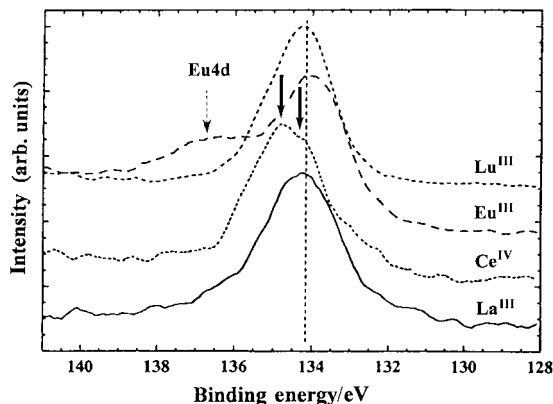
Fig. 7 Core-level spectra for the P2p orbital of DPP in the La^{III}, Ce^{IV}, Eu^{III}, and Lu^{III} complexes. [Lanthanide ion]$_0$ / [DPP]$_0$ = 10. The two bold arrows correspond to the P_H and P_L in Fig. 9.

ently, the Ce^{IV} ion exceeds the other metal ions in electron-withdrawing activity, and exceptionally promotes the electrophilicity of the phosphodiester linkage. The superiority of Ce^{IV} for the activation of DNA has been for the first time spectroscopically studied.

According to the L_3-XANES spectroscopy, 0.67 electrons exist in the 4f-orbitals of the Ce ion in the Ce^{IV}–DPP complex (these orbitals should be empty, if the Ce were to be really tetravalent). Upon complex formation, the electrons flow into the 4f-orbitals from the surroundings. In the DPP complexes of Ce^{III} and other lanthanide(III) ions, however, the corresponding electron-transfer to the metal(III) ions is not observed. The enormous activity of Ce^{IV} for DNA hydrolysis is primarily ascribed to the dominant electron-accepting activity, which is derived from the stability of its trivalent state. The lanthanide(III) ions cannot efficiently accept the electrons from DNA, since their divalent states are too unstable.

(2) Mixing of the orbitals of the phosphodiester linkage with those of Ce^{IV}. The electron-transfer from the phosphate to the Ce^{IV} ion occurs, at least partially, through the hybrid orbitals, which are formed from the 4f-orbitals of Ce^{IV} and the orbitals of the phosphorus atom (and/or of the oxygen atom) in the phosphate residue.[24] Consistently, a new energy state, related to this hybrid 4f-orbitals, appears near the Fermi level, when the Ce^{IV}–DPP complex is formed (Fig. 8). Neither free
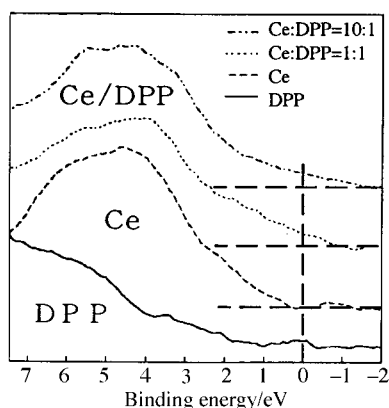

Fig. 8 X-Ray photoelectron spectra near the Fermi level.

DPP nor the Ce^{IV} hydroxo cluster (without DPP) has any energy-state density at this level. Since the 4f-orbitals of Ce^{IV} are lower in energy than those of the lanthanide(III) ions, and, at the same time, are widely spreading in space, they can efficiently interact with the orbitals of the phosphate. This mixing of the orbitals (as well as the resultant electron-transfer)

would be still more efficient in the transition state, and decrease the activation free energy for the DNA hydrolysis.

(3) Structure of the Ce^{IV}–phosphate complex. According to detailed analysis of the core-level spectra, the phosphodiester is simultaneously coordinated to two Ce^{IV} ions, and enormously activated. As depicted in Fig. 9, the P2p signals of DPP in the
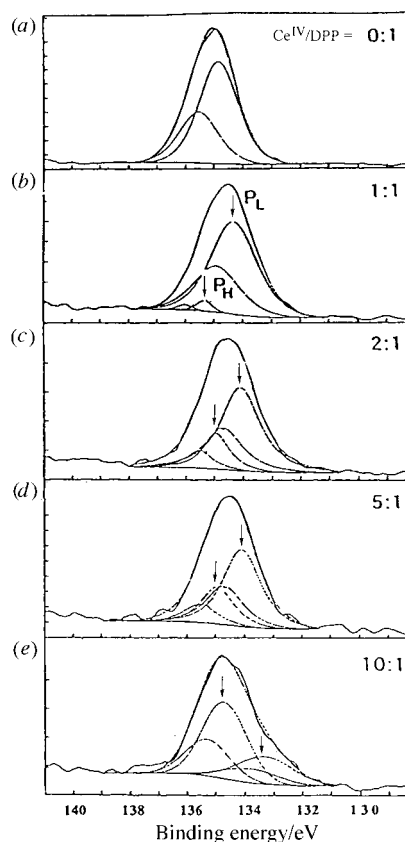

Fig. 9 Core-level spectra of the P2p orbital of DPP in the Ce^{IV}–DPP mixtures of different molar ratios. The peaks P_H and P_L correspond to the doublet signals of higher and lower binding energies.

Ce^{IV} complexes are composed of two components (P_H and P_L: each of the peaks is further split into a spin doublet). When the Ce^{IV}:DPP ratio is 1:1, the peak P_L of lower energy is predominant (b). Here, the phosphodiester linkage is bound to one Ce^{IV} ion and is only slightly activated (DNA hydrolysis hardly takes place). As the Ce^{IV}:DPP ratio increases [Fig. 9(c)–(e)], the intensity of P_H (of higher energy) gradually increases. This signal corresponds to DPP which is coordinated to two Ce^{IV} ions in the hydroxo cluster and is exceptionally activated by 'two-metal activation' (see Fig. 11). Consistently, the remarkable DNA hydrolysis occurs when Ce(IV) exists in excess to DNA.

These arguments are further substantiated by the EXAFS spectra in Fig. 10. In the absence of DPP [Fig. 10(a), (b)] the Ce^{IV} ions form metal hydroxo clusters (and the gel as their aggregates). Accordingly, the signal for the Ce–Ce distance is clearly observed at 3.6 Å (the position designated by the broken line). The signal at around 2.0 Å is for the Ce–O distance. Upon addition of DPP, the Ce–Ce signal rapidly weakens and is virtually nil at a Ce:DPP ratio of 1:1 [Fig. 10(c)]. Since the 1:1 Ce^{IV}–DPP complexes exist independently from each other (without mutual aggregation), the Ce–Ce signal is absent. When the Ce^{IV}:DPP ratio is >1, however, the Ce–Ce signal appears again and gradually increases with increasing Ce:DPP ratio [Fig. 10(d), (e)]. Here, two Ce^{IV} ions are simultaneously interacting with one DPP molecule, and located in close
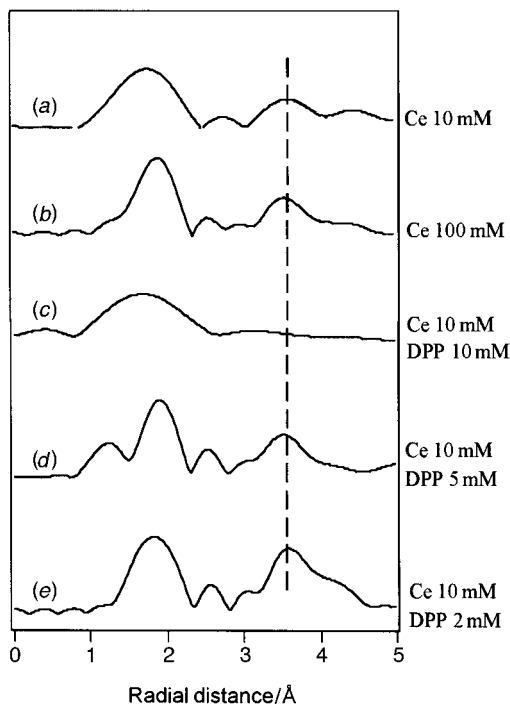
Fig. 10 EXAFS spectra for the Ce^{IV}–DPP systems.

proximity. Thus, these two Ce^{IV} ions are bound to each other, giving rise to the Ce–Ce signal.

1.6 Proposed mechanism for the DNA hydrolysis

The proposed mechanism is schematically depicted in Fig. 11. First, the phosphate residue is coordinated to the two Ce^{IV} ions in [Ce$^{IV}_2$(OH)$_4$]$^{4+}$ (the apparent association constant between Ce^{IV} and TpT is 10^3 M^{-1} at pH 2 and 50 °C).[9] As the result, the electrons of the phosphate are strongly withdrawn by the Ce^{IV} ions. Furthermore, the orbitals of the phosphate are mixed with the 4f-orbitals of Ce^{IV}, and form new hybrid orbital(s). These two factors greatly activate the phosphodiester linkage for the nucleophilic attack.

Then, the phosphate is attacked by the hydroxide ion coordinated to one of the two Ce^{IV} ions. According to the potentiometric titration, each of the Ce^{IV} ions releases three protons from its coordinated water to the aqueous phase, when the pH is increased from 0 to 4 (no proton is released above pH 4). Although this metal-bound hydroxide ion is a rather weak nucleophile, the phosphate is so activated (as described above) that the reaction can efficiently proceed. Furthermore, the hydroxide ion is located at quite a suitable position for the nucleophilic attack (the two Ce^{IV} ions in the bimetallic cluster
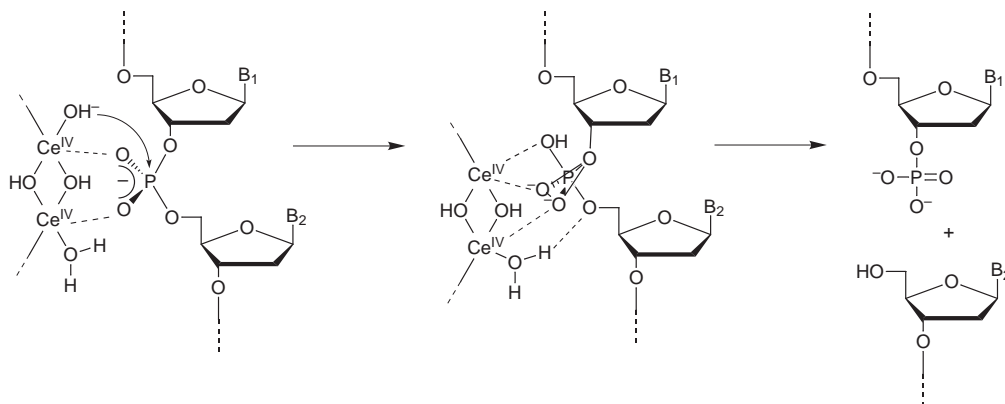
have many coordinated water molecules, and at least one of them is placed appropriately for the purpose). Finally, the positive charges, accumulated in the Ce^{IV} hydroxo cluster (and also in the hydroxide gel as their aggregates), stabilize the negatively-charged transition state of DNA hydrolysis (the transition state is more negatively charged than the initial state, and is stabilized to a greater extent by the adjacent positive charges). Because of these factors, the pentacoordinated intermediate is efficiently formed.

In the breakdown of the intermediate, the water bound to Ce^{IV} functions as an acid catalyst. With this catalysis, the alkoxide ion of the 5′-OH of the 2′-deoxyribonucleotide (which is otherwise very unstable) can be promptly removed from the phosphorus atom. The large coordination number of the Ce^{IV} ions in the bimetallic cluster is favorable for the catalysis, exactly as described above for the first-step of DNA hydrolysis. The notable D$_2$O solvent isotope effect (see the Section 1.1) is associated with this proton transfer.

These arguments are supported by the fact that the activity of Ce^{IV} for DNA hydrolysis is substantially enhanced by cooperation with Pr^{III}.[25] When the Ce^{IV} : Pr^{III} ratio is 2, the activity is 10 fold greater than that of the Ce^{IV} ion (the Pr^{III} itself is virtually inactive under the reaction conditions employed). The catalysis occurs in the mixed hydroxo clusters, formed from these two metal ions in the reaction mixtures. Presumably, the Pr^{III} ion in this mixed cluster provides its metal-bound water as the acid catalyst, and promotes the second-step of DNA hydrolysis (the removal of the 5′-OH of 2′-deoxyribonucleotide). Under the reaction conditions (around pH 7), the Pr^{III}-bound water mostly remains undissociated (pK_a ~ 9),[26] and is superior as an acid catalyst to the Ce^{IV}-bound water. Although the [Ce^{IV}(H$_2$O)$_n$]$^{4+}$ ion is intrinsically a very strong acid (the pK_a for the first deprotonation is around 0),[26] it loses three protons at pH 0–4, and is only a weak acid at pH 7.[27]

On the CeCl$_3$-induced DNA hydrolysis under air, a mechanism, in which a hydrogen peroxide-like species (formed by the reduction of O$_2$ with the Ce^{III}) functions as the nucleophile, was proposed.[8b] However, this mechanism is unlikely, since Ce^{IV} salts satisfactorily hydrolyse DNA even in the complete absence of O$_2$.[8a,9] The role of O$_2$ is only to oxidize the Ce^{III} to the catalytically active Ce^{IV}, and not to provide the nucleophile. The nucleophile comes from the water.
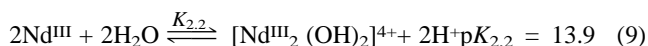
2 Lanthanide(III) ion-induced hydrolysis of RNA

Since RNA has the 2′-OH of ribose as an intramolecular nucleophile towards the phosphorus atom, RNA is far more promptly (10^5–10^6 fold) hydrolysed than is DNA. Yet, non-enzymatic hydrolysis of RNA under physiological conditions is not easy (in order to hydrolyse RNA within an hour, for example, the catalyst must accelerate the reaction by 10^7-fold or more). Although a number of catalysts have been proposed,

Fig. 11 Proposed mechanism of the Ce^{IV}-induced DNA hydrolysis [the P–O(5′) scission is presented here, although the P–O(3′) scission can also occur (see ref. 15)].

none of them exceeds (or is even comparable with) the lanthanide(III) ions in activity.

The catalytic activity of the lanthanide(III) ions at pH 7 monotonically increases with increasing atomic number.[10] With the last three (Tm[III], Yb[III], and Lu[III]), RNA hydrolysis is completed within a few minutes at pH 7 and 30 °C. Interestingly, Ce[IV], which is the best for DNA hydrolysis, is not so active for RNA hydrolysis (its activity is comparable with that of Tb[III]).

2.1 Catalytic species for RNA hydrolysis

The solvolysis chemistry of Nd[III] is well known [eqn. (8) and (9)].[28] Thus, the Nd[III]-induced hydrolysis of adenylyl(3′-5′)adenosine (ApA) has been kinetically analyzed in detail.[10] In

$$Nd^{III} + H_2O \xrightleftharpoons{K_{1,1}} [Nd^{III}(OH)]^{2+} + H^+ \quad pK_{1,1} = 9.4 \quad (8)$$

$$2Nd^{III} + 2H_2O \xrightleftharpoons{K_{2,2}} [Nd^{III}_2(OH)_2]^{4+} + 2H^+ \quad pK_{2,2} = 13.9 \quad (9)$$

the reaction mixtures, there exist three Nd[III]-derived species: free Nd^{3+}, $[Nd^{III}(OH)]^{2+}$, and $[Nd^{III}_2(OH)_2]^{4+}$. The equilibrium concentration of each species can be calculated by using the $K_{1,1}$ and $K_{2,2}$ values.

As shown in Fig. 12, the logarithm of the rate of RNA hydrolysis steeply increases with increasing pH, up to pH 8, and
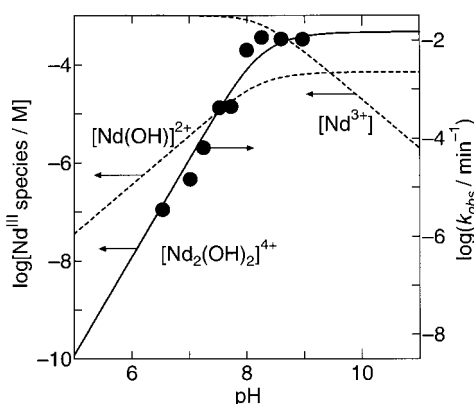
Fig. 12. The pH dependence of the rate of ApA hydrolysis by NdCl₃ (1 mM) at 30 °C. The closed circles are the experimental points, whereas the curved lines show the equilibrium concentration of the Nd[III]-derived species.

then attains a plateau. The experimental points fit well the theoretical line showing the equilibrium concentration of $[Nd^{III}_2(OH)_2]^{4+}$ (the solid line). This bimetallic cluster is the active species for RNA hydrolysis (its formation is accompanied by the release of two protons, as shown by eqn. (9), and thus the pH–rate constant profile is so steep). This conclusion is further supported by the dependence of hydrolysis rate on the initial concentration of Nd[III]Cl₃. In order to hydrolyse RNA efficiently, the bimetallic structure is essential. This finding is totally consistent with the fact that $[Ce^{IV}_2(OH)_4]^{4+}$ is the active species for Ce[IV]-induced DNA hydrolysis.

2.2 Why does the activity of the lanthanide(III) ion at pH 7 increase with increasing atomic number?

The pH–rate constant profiles for all the lanthanide(III) ions have similar shapes, and are composed of (a) a steep straight line at lower pH and (b) a plateau at higher pH (see Fig. 13). The straight line corresponds to the formation of the active species $[Ln^{III}_2(OH)_2]^{4+}$ (Ln = lanthanide ion), whereas its formation is completed in the plateau.

As the atomic number increases, these profiles gradually shift towards the lower pH side. Accordingly, the concentration of the active species at pH 7 increases in this order. For example, Lu[III] exists mostly as the bimetallic active species ($[Lu^{III}_2(OH)_2]^{4+}$) at pH 7. As the result, this metal ion is quite
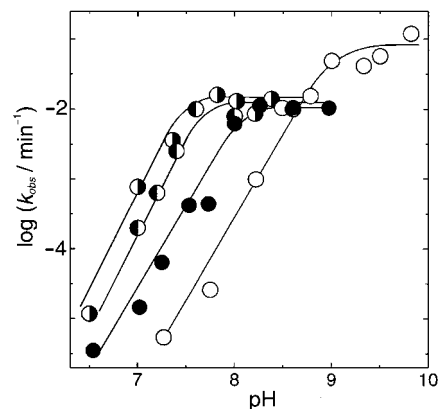
Fig. 13 The pH dependence of the rate of ApA hydrolysis by various lanthanide(III) chlorides (1 mM) at 30 °C: (◯) La[III], (●) Nd[III], (◐) Tb[III], (◑) Lu[III]. Only the typical results are presented here, since the shapes of the profiles for all the lanthanide(III) ions are similar and their positions monotonically shift towards lower pH side with increasing atomic number.

active for RNA hydrolysis in neutral solutions. For La[III], however, only a small fraction takes the active form at pH 7. Thus, Tm[III], Yb[III], and Lu[III] are superior to the others, when the RNA hydrolysis is carried out under physiological conditions. In alkaline solutions, even the La[III] ion mostly takes the active form and is sufficiently active.[29]

2.3 The rate-limiting step for RNA hydrolysis

When the 5′-O atom in RNA is replaced with a sulfur, the rate of alkaline hydrolysis of the corresponding phosphodiester linkage is increased by 10⁵–10⁶ fold.[30] Exactly as discussed in DNA hydrolysis (Section 1.2), the removal of the 5′-OH of the ribose from the phosphorus atom is rate limiting. Similarly, the lanthanide ion-induced RNA hydrolysis involves a rate-limiting removal of the 5′-OH.[10,31]

Based on these results, the energy diagrams are depicted in Fig. 4(b). The lanthanide(III) ions primarily accelerate the second step (the removal of the 5′-OH). At the same time, however, the first step (the intramolecular attack by the 2′-OH towards the phosphorus atom) is also promoted, to some extent (> 10²⁻³ fold), so that the second-step remains rate-limiting (the RNA hydrolysis is accelerated by 10⁸ fold). It is noteworthy that the first barrier in the alkaline hydrolysis of RNA is much lower than that in DNA hydrolysis [compare Fig. 4(a) with 4(b)]. The intramolecular attack by the 2′-OH is enormously efficient compared with the intermolecular reaction in the latter. Furthermore, the second barrier in the RNA hydrolysis (corresponding to $\Delta G_2^{\ddagger}$) is considerably higher than the first barrier (the rate difference is 10⁵–10⁶ fold). This is in contrast with the symmetric energy diagram in the DNA hydrolysis. The RNA hydrolysis involves the formation of a 2′,3′-cyclic monophosphate of the ribonucleotide as the first product, and a considerable strain is induced on the formation of this five-membered ring phosphate. The cyclic phosphate is much more reactive than RNA, and is rapidly hydrolysed to the 2′- or 3′-monophosphate as the final product.

2.4 Proposed mechanism of the RNA hydrolysis

First, the phosphodiester linkage in RNA is coordinated to the lanthanide(III) ion in the bimetallic cluster $[Ln^{III}_2(OH)_2]^{4+}$. In the following intramolecular nucleophilic attack by the 2′-OH towards the phosphorus atom, the hydroxide ion, bound to the metal ion(s), functions as the general base catalyst. Alternatively, the 2′-OH is directly coordinated to the metal ion, and its dissociation to alkoxide ion is facilitated.

In the breakdown of the resultant pentacoordinated intermediate, the metal-bound water (or the metal ion itself)

functions as the general acid catalyst. The water bound to the lanthanide(III) ions has a pK_a of around 8–9, which should be further decreased in the bimetallic clusters through the electron-withdrawal by the second metal(III) ion. This is quite appropriate for the present acid catalysis, since the RNA hydrolysis is carried out at around pH 7 (when the apparent activities of various acid catalysts are compared with each other at a predetermined pH, the activity increases as the pK_a gets closer to the pH).[31] The acid catalysis cooperates with the base catalysis in the hydroxo clusters, resulting in the prompt hydrolysis of RNA (Fig. 14).
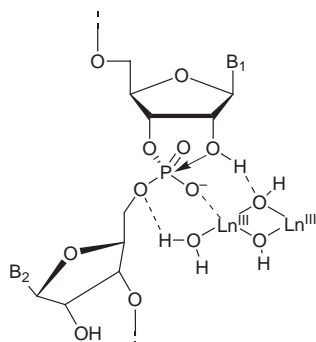

Fig. 14 Proposed mechanism of the lanthanide(III)-induced RNA hydrolysis.

3 DNA hydrolysis *vs.* RNA hydrolysis

What factor makes the Ce^{IV} ion the best for DNA hydrolysis? Why does RNA hydrolysis choose the lanthanide(III) ions? The energy diagrams in Fig. 4 give us some tips on these subjects. The energy diagram for the uncatalysed (alkaline) hydrolysis of DNA is virtually symmetric, and the heights of the first barrier and the second barrier are almost the same [the dotted line in Fig. 4(*a*)]. Under these conditions, the primary requirement for efficient catalysis is to *lower the energy barrier of the first step* (otherwise, the first barrier governs the rate of the whole reaction, no matter how much the second step is promoted). Second, the catalyst must stabilize the pentacoordinated intermediate with respect to the initial state [see eqn. (1)]. The Ce^{IV} ion satisfactorily fulfils these requirements, through the activation of the DNA by both (a) withdrawing the electrons from the phosphate in the 'two-metal activation' (Fig. 7 and 9) and (b) mixing its f-orbitals with those of the phosphate (Fig. 8). The second barrier is lowered with respect to the initial state, mainly because ΔG_1 is decreased. In contrast, the lanthanide(III) ions cannot activate DNA to such an extent that they are rather poor for DNA hydrolysis.

In uncatalysed hydrolysis of RNA [Fig. 4(*b*)], however, the second energy barrier is far higher than is the first energy barrier (10^5–10^6 fold difference in the reaction rate), as described in Section 2.3. Here, the promotion of the second step should directly accelerate the whole reaction (until it becomes lower than the first barrier). The promotion of the first step is not as essential as is the case in DNA hydrolysis. The lanthanide(III) ions are suitable for the acid catalysis in the second step, since they have many (8 or 9) coordinated water molecules and their pK_a values are close to the pH of the reaction mixtures (*vide ante*).[32]

4 From lanthanide ions to non-lanthanide ions

Soon after the remarkable catalysis by the lanthanide ions was discovered, many laboratories attempted to hydrolyse DNA and RNA by using non-lanthanide ions.[1] These catalysts, if available, should be useful for various practical applications (especially *in vivo*). It has been established that RNA can be hydrolysed by these metal ions, if two (or more) of them

satisfactorily cooperate in dinuclear (or multi-nuclear) complexes (to date, there are no non-lanthanide complexes which can hydrolyse DNA of various sequences and structures).[33] In order to place the metal ions appropriately, various ligands have been designed. The control of acid/base properties of the metal ions (and of the water bound to them) is also important. For example, Zn^{II} ion itself is virtually inactive for RNA hydrolysis at pH 7. Mono-nuclear Zn^{II} complexes also exhibit poor activity. However, di- and tri-nuclear Zn^{II} complexes of pyridine-based ligands efficiently hydrolyse RNA (Fig. 15).[34,35] By attaching these zinc(II) complexes to DNA oligomers, sequence-selective artificial ribonucleases have been synthesized.[36]
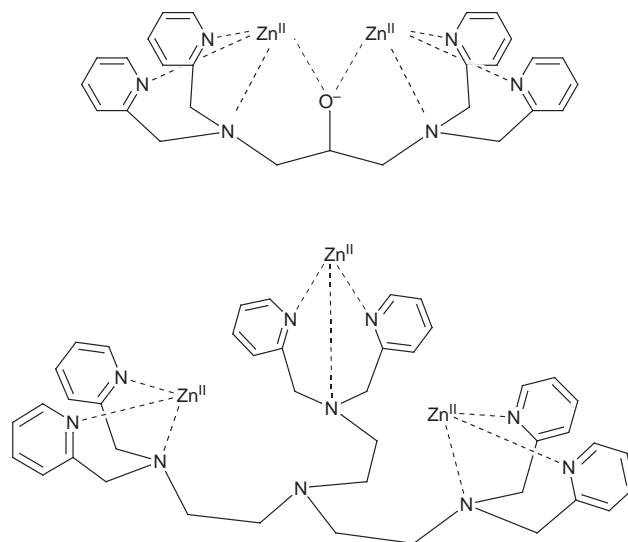

Fig. 15. Di- and tri-nuclear Zn^{II} complexes for RNA hydrolysis.

The lanthanide ions spontaneously form multi-nuclear clusters under physiological conditions, even in the absence of specific ligands. Two or more lanthanide ions are appropriately placed in these clusters, where bimetallic (or multi-metallic) synergism efficiently takes place. The 4f-orbitals activate the phosphates through orbital–orbital interactions. Furthermore, the acid/base properties of the coordinated water on the lanthanide ions are suitable for the catalysis at pH 7. Finally, the positively-charged reaction field, provided by the clusters, stabilizes the negatively-charged transition states for the hydrolysis of DNA and RNA. The combination of these factors gives rise to the remarkable activities of the lanthanide ions.

Conclusions

A few years ago, it was found that the lanthanide ions hydrolyse DNA and RNA under physiological conditions, and we have obtained useful tools to manipulate DNA and RNA without using naturally-occurring enzymes. However, the mechanistic details of these remarkable catalyses were not clear. In the present study, the following important conclusions have been obtained on the mechanisms of these catalyses.

(1) Tetracationic bimetallic hydroxo clusters are the active species ([Ce$^{IV}_2$(OH)$_4$]$^{4+}$ for DNA hydrolysis and [Ln$^{III}_2$(OH)$_2$]$^{4+}$ for RNA hydrolysis).

(2) The Ce^{IV} ion notably activates the phosphodiester linkages in DNA to nucleophilic attack, through (a) electron-withdrawal from the residues and (b) mixing its 4f-orbitals with their orbitals. As a result, the formation of the pentacoordinated intermediate is remarkably promoted.

(3) The catalysis for RNA hydrolysis is mainly ascribed to the acceleration of the breakdown of the pentacoordinated intermediate. The activity at pH 7 increases with increasing atomic number of the lanthanide(III) ion, since the concentration of the

active species (the bimetallic hydroxo cluster) increases in this order.

(4) In the lanthanide-induced hydrolysis of both DNA and RNA, the breakdown of the pentacoordinated intermediate is rate limiting.

These findings are valuable for the design of still more advanced catalysts for the hydrolysis of DNA and RNA, as well as artificial enzymes for site-selective scission of them. What should be clarified next is (1) what is the real nature of the orbital-mixing between the Ce^{IV} ion and the phosphate? and (2) how big a contribution is made to DNA activation by each of the electron-withdrawal and the orbital-mixing? In order to solve these problems, quantum-chemical analyses are under way. The application of lanthanide catalysis to biotechnology, molecular biology, and therapy are also currently being attempted.

Acknowledgements

Notes and references

1 Recent reviews: M. Komiyama and J. Sumaoka, *Curr. Opin. Chem. Biol.*, 1998, **2**, 751; M. Oivanen, S. Kuusela and H. Lönnberg, *Chem. Rev.*, 1998, **98**, 961; B. N. Trawick, A. T. Daniher and J. K. Bashkin, *Chem. Rev.*, 1998, **98**, 939; G. Pratviel, J. Bernadou and B. Meunier, in *Advances in Inorganic Chemistry*, ed. A. G. Sykes, Academic Press, San Diego, 1998, vol. 45, p. 251; D. M. Perreault and E. V. Anslyn, *Angew. Chem., Int. Ed. Engl.*, 1997, **36**, 432; J. Chin, *Curr. Opin. Chem. Biol.*, 1997, **1**, 514; E. Kimura and T. Koike, in *Advances in Inorganic Chemistry*, ed. A. G. Sykes, Academic Press, San Diego, 1997, vol. 44, p. 229 and references cited therein.
2 The scission site of a restriction enzyme, which recognizes a sequence of 6 DNA bases, appears every 4^6 DNA bases (in average). If the DNA of the human beings, composed of more than 10^9 DNA bases, is treated with this restriction enzyme, the scission occurs at more than 10^5 sites.
3 The half-life of the phosphodiester linkage in DNA at pH 7 and 30 °C is estimated to be 200 million years. Although the linkage in RNA is much more reactive than that in DNA, its half-life is still 1000 years or so.
4 Supercoiled DNA, which is activated by strain and other factors, was reportedly cleaved *via* the hydrolytic pathway: L. A. Basile, A. L. Raphael and J. K. Barton, *J. Am. Chem. Soc.*, 1987, **109**, 7550; L. M. T. Schnaith, R. S. Hanson and L. Que, Jr., *Proc. Natl. Acad. Sci. U.S.A.*, 1994, **91**, 569; S. Hashimoto and Y. Nakamura, *J. Chem. Soc., Perkin Trans. 1*, 1996, 2623; R. Hettich and H.-J. Schneider, *J. Am. Chem. Soc.*, 1997, **119**, 5638.
5 DNA hydrolysis: Y. Matsumoto and M. Komiyama, *Nucleic Acids Symp. Ser.*, 1992, **27**, 33; M. Komiyama, K. Matsumura, K. Yonezawa and Y. Matsumoto, *Chem. Express*, 1993, **8**, 85; T. Shiiba, K. Yonezawa, N. Takeda, Y. Matsumoto, M. Yashiro and M. Komiyama, *J. Mol. Catal.*, 1993, **84**, L21.
6 RNA hydrolysis: K. Matsumura and M. Komiyama, *J. Chem. Soc., Chem. Commun.*, 1992, 640; J. R. Morrow, L. A. Buttrey, V. M. Shelton and K. A. Berback, *J. Am. Chem. Soc.*, 1992, **114**, 1903; J. R. Morrow and V. M. Shelton, *New J. Chem.*, 1994, **18**, 371; R. Breslow and D.-L. Huang, *Proc. Natl. Acad. Sci. U.S.A.*, 1991, **88**, 4080.
7 On the hydrolysis of various activated phosphoesters, see ref. 1.
8 (*a*) M. Komiyama, T. Shiiba, T. Kodama, N. Takeda, J. Sumaoka and M. Yashiro, *Chem. Lett.*, 1994, 1025; (*b*) B. K. Takasaki and J. Chin, *J. Am. Chem. Soc.*, 1994, **116**, 1121.
9 M. Komiyama, N. Takeda, Y. Takahashi, H. Uchida, T. Shiiba, T. Kodama and M. Yashiro, *J. Chem. Soc., Perkin Trans. 2*, 1995, 269.
10 K. Matsumura and M. Komiyama, *J. Biochem.*, 1997, **122**, 387.
11 Sequence-selective DNA scission: M. Komiyama, T. Shiiba, Y. Takahashi, N. Takeda, K. Matsumura and T. Kodama, *Supramol. Chem.*, 1994, **4**, 31; M. Komiyama, N. Takeda, T. Shiiba, Y. Takahashi, Y. Matsumoto and M. Yashiro, *Nucleosides Nucleotides*, 1994, **13**, 1297; M. Komiyama, *J. Biochem.*, 1995, **118**, 665.

12 Sequence-selective RNA scission: K. Matsumura, M. Endo and M. Komiyama, *J. Chem. Soc., Chem. Commun.*, 1994, 2019; J. Hall, D. Hüsken and R. Häner, *Nucleosides Nucleotides*, 1997, **16**, 1357; D. Magda, M. Wright, S. Crofts, A. Lin and J. L. Sessler, *J. Am. Chem. Soc.*, 1997, **119**, 6947.
13 J. Sumaoka, Y. Azuma and M. Komiyama, *Chem. Eur. J.*, 1998, **4**, 205.
14 N. Takeda, Y. Okada and M. Komiyama, unpublished results.
15 The electrophilicity of the phosphorus atom is not much altered by the $O \rightarrow S$ substitution, since the substitution of non-bridging oxygen in the phosphate to sulfur hardly affects the rate of hydrolysis. In Tp-OCH$_2$CF$_3$, the perturbation on the phosphorus atom is still smaller. In the Ce^{IV}-induced hydrolysis of Tp-OT, the P–O(3′) bond and the P–O(5′) bond are cleaved at almost the same rates (the resultant 5′- and 3′-monophosphates of thymidine are rapidly hydrolysed to thymidine as the final product, and thus are not much accumulated: see ref. 9). In the hydrolysis of Tp-ST and Tp-OCH$_2$CF$_3$, the P–S bond and P–O(5′) bond are exclusively cleaved.
16 Homogeneous hydrolysis of DNA at pH 7 by Ce^{IV}–saccharide complexes was reported: A. Kajimura, J. Sumaoka and M. Komiyama, *Carbohydr. Res.*, 1998, **309**, 345.
17 F. B. Charles Jr. and R. E. Mesmer, *The Hydrolysis of Cations*, Wiley, New York, 1976, p. 138.
18 J. Sumaoka, N. Takeda, Y. Okada, H. Takahashi, H. Shigekawa and M. Komiyama, *Nucleic Acids Symp. Ser.*, 1998, **39**, 137.
19 J. Sumaoka, K. Furuki and M. Komiyama, unpublished results.
20 J. Sumaoka, S. Miyama and M. Komiyama, *J. Chem. Soc., Chem. Commun.*, 1994, 1755.
21 H. Shigekawa, H. Ikawa, R. Yoshizaki, Y. Iijima, J. Sumaoka and M. Komiyama, *Appl. Phys. Lett.*, 1996, **68**, 1433.
22 H. Shigekawa, M. Ishida, K. Miyake, R. Shioda, Y. Iijima, T. Imai, H. Takahashi, J. Sumaoka and M. Komiyama, *Appl. Phys. Lett.*, 1999, **74**, 460.
23 The EXAFS and XANES measurements were carried out on samples frozen in liquid nitrogen.
24 Various characteristic properties of Ce compounds have been interpreted in terms of the formation of similar hybrid orbitals. For example, CeRu$_2$, CeCo$_2$, and CeRh$_3$ are non-magnetic, but show 4f-derived emission in their resonant photoemission spectra. Apparently, the 4f character is delocalized by the hybridization. The number of 4f electrons should be between 0 and 1 depending on the amount of the charge-transfer: A. Fujimori, *Phys. Rev. B*, 1983, **28**, 4489; A. Bianconi, H. Marcelli, R. Dexpert, A. Karnatak, T. J. Kotani and J. Petiau, *Phys. Rev. B*, 1987, **35**, 806 and references cited therein.
25 N. Takeda, T. Imai, M. Irisawa, J. Sumaoka, M. Yashiro, H. Shigekawa, and M. Komiyama, *Chem. Lett.*, 1996, 599. This Ce^{IV}/Pr^{III} combination is the most active catalyst for DNA hydrolysis ever reported.
26 J. Burgess, *Metal Ions in Solution*, Wiley, New York, 1978, p. 267.
27 Alternatively, Pr^{III} can provide its metal-bound hydroxide as the nucleophile. The hydroxide is a better nucleophile than the Ce^{IV}-bound hydroxide.
28 K. A. Burkov, L. S. Lilich, N. D. Ngo and A. Yu. Smirnov, *Russ. J. Inorg. Chem.*, 1973, **18**, 797.
29 P. Hurst, B. K. Takasaki and J. Chin, *J. Am. Chem. Soc.*, 1996, **118**, 9982.
30 X. Liu and C. B. Reese, *Tetrahedron Lett.*, 1995, **36**, 3413; J. B. Thomson, B. K. Patel, V. Jimenez, K. Eckart and F. Eckstein, *J. Org. Chem.*, 1996, **61**, 6273; R. G. Kuimelis and L. W. McLaughlin, *Nucleic Acids Res.*, 1995, **23**, 4753; D.-M. Zhou, N. Usman, F. E. Wincott, J. Matulic-Adamic, M. Orita, L.-H. Zhang, M. Komiyama, P. K. R. Kumar and K. Taira, *J. Am. Chem. Soc.*, 1996, **118**, 5862.
31 T. Shiiba and M. Komiyama, *Tetrahedron Lett.*, 1992, **33**, 5571.
32 The Brønsted relationship indicates that the intrinsic activity of acid catalysts increases with decreasing pK_a. However, the concentration of the active species (in the acidic form) at a predetermined pH decreases in this order. Thus, the net efficiency of the catalysis, determined by (the intrinsic activity of active species) $\times$ (the concentration of active species), takes the maximum when the pK_a is close to the reaction pH (see M. L. Bender, R. J. Bergeron and M. Komiyama, *The Bioorganic Chemistry of Enzymatic Catalysis*, Wiley, New York, 1984, ch. 6.
33 Some of the complexes in ref. 4 were proposed to be active for the hydrolysis of non-supercoiled DNA.
34 M. Yashiro, A. Ishikubo and M. Komiyama, *J. Chem. Soc., Chem. Commun.*, 1995, 1793.
35 M. Yashiro, A. Ishikubo and M. Komiyama, *J. Chem. Soc., Chem. Commun.*, 1997, 83.
36 S. Matsuda, A. Ishikubo, A. Kuzuya, M. Yashiro and M. Komiyama, *Angew. Chem., Int. Ed.*, 1998, **37**, 3284.

Paper 9/01621J